

Synthesis, structure and catecholase-like activity of a new dicopper(II) complex with benzoylacetate ligand

József Kaizer^a, Róbert Csonka^b, Gábor Speier^{a,b,*}, Michel Giorgi^c,
Marius Réglér^c

^a *Research Group for Petrochemistry, Hungarian Academy of Sciences, 8200 Veszprém, Hungary*

^b *Department of Organic Chemistry, University of Veszprém, 8200 Veszprém, Hungary*

^c *Laboratoire de Cristallographie et Laboratoire de Bioinorganique Structurale, Université Paul Cézanne Aix-Marseille III, F.S.T. Saint-Jérôme, Service 432, Avenue Escadrille Normandie-Niemen, 13397 Marseille Cedex 20, France*

Received 8 December 2004; received in revised form 3 March 2005; accepted 3 March 2005

Abstract

The preparation and characterization of tetranuclear $\text{Cu}_4(\text{bnac})_4(\mu\text{-OEt})_4$ complex is described. Crystallographic characterization of this complex has shown that the co-ordination geometry around copper(II) ions is distorted square pyramidal (monoclinic, $C2/c$, $a = 13.3980(2)$ Å, $b = 14.6080(2)$ Å, $c = 25.7460(4)$ Å, $\alpha = 90.00^\circ$, $\beta = 103.4090(10)^\circ$, $\gamma = 90.00^\circ$, $V = 4901.59(13)$ Å³, $Z = 8$). The in situ-generated $\text{Cu}_2(\text{bnac})_2(\mu\text{-OEt})_4(4\text{R-py})_4$ complexes were suitable catalysts for the catalytic oxidation of 3,5-DTBCH₂ to 3,5-DTBQ with dioxygen at ambient condition in good yields. The catalytic activity was found to obey Michaelis–Menten type kinetics and increase with electron-releasing substituent on co-ordinated pyridines.

© 2005 Elsevier B.V. All rights reserved.

Keywords: Copper; Catecholase activity; Oxygenation; X-ray structure

1. Introduction

The synthesis and reactivity studies of bimetallic copper(II) complexes, as model compounds for metalloenzymes with oxidase activity, is of particular interest for the development of bioinspired catalysts for oxidation reactions. The dicopper proteins hemocyanin, tyrosinase and catechol oxidase have been shown to contain a coupled binuclear metal center. Despite the similar geometric and electronic structures of their dicopper centers, these proteins carry out different biological functions: hemocyanin is the oxygen transport and storage protein in arthropods and molluscs and tyrosinase catalyzes the *ortho*-hydroxylation of phenols with further oxidation of the catechol product to the *o*-quinone. Catechol oxidase (EC 1.10.3.1), forms the third member of this group of type 3 copper proteins [1–4]. Catechol

oxidases, in contrast to tyrosinases, catalyze exclusively the oxidation of catechols to the corresponding *o*-quinones without acting on monophenols [5]. The structures of oxidized and reduced forms of catechol oxidase from sweet potato were determined by X-ray crystallography [6–8]. Both consist of a binuclear copper center each co-ordinated by three histidine nitrogen atoms. This reaction is of great importance in medical diagnosis for the determination of the hormonally active catecholamines adrenaline, noradrenaline and dopa [9]. In the oxidized catechol oxidase structure, the two cupric ions are 2.9 Å apart. In addition to the six histidine ligands, a bridging solvent molecule, most likely a hydroxide ion completing the four-co-ordinate trigonal pyramidal co-ordination sphere for both cupric metal ions. EPR data reflect an antiferromagnetically coupled EPR silent Cu(II)–Cu(II) state of the enzyme in agreement with a solvent molecule bridging the copper atoms observed in the crystal structure [10]. The catecholase activity of synthetically prepared copper compounds with different structural

* Corresponding author. Tel.: +36 88 422 0224657; fax: +36 88 427 492.
E-mail address: speier@almos.vein.hu (G. Speier).

parameters has been investigated to some extent [11–18]. It has been assumed that geometry around the copper ions, intermetallic distance, lability of exogenous ligands and electrochemical properties are the main key factors that determine the catecholase-like activity of the complexes.

In addition to former kinetic studies on catechol oxidase model systems [19–21] in this paper we report the synthesis of a series of binuclear copper(II) complexes $\text{Cu}_2(\text{bnac})_2(\mu\text{-OEt})_4(4\text{R-py})_4$ (generated from the tetranuclear $\text{Cu}_4(\text{bnac})_4(\mu\text{-OEt})_4$ complex by the use of 4-substituted pyridines) as potential structural and functional models for the active sites of catechol oxidase. The catecholase activity of these binuclear compounds have been measured in order to get insight into the possible role of the basicity of donating, nitrogen-containing ligands.

2. Experimental

2.1. Materials

All manipulations were performed under a pure dinitrogen or argon atmosphere unless otherwise stated, using standard Schlenck-type inert-gas techniques [22]. Solvents used for the reactions were purified by literature methods [23] and stored under argon. $\text{Cu}(\text{OMe})_2$ was prepared according to the literature [24]. All other chemicals were commercial products and were used as received without further purification.

2.2. Analytical measurements

Infrared spectra were recorded on a Specord 75 IR (Carl Zeiss) spectrophotometer using samples muller in Nujol between KBr plates or in KBr pellets. UV–vis spectra were recorded on a Shimadzu UV-160 spectrophotometer using quartz cells. Microanalyses were done by the Microanalytical Service of the University.

2.3. Synthesis of $\text{Cu}_4(\text{bnac})_4(\mu\text{-OEt})_4$

A solution of 162 mg (1 mmol) of benzoylacetone in 5 cm^3 ethanol was added to a solution of 125 mg (1 mmol) $\text{Cu}(\text{OMe})_2$ in 5 cm^3 ethanol. The resulting blue solution was heated at 343 K for 2 h, filtered and kept for slow evaporation to obtain crystals suitable for X-ray structure determination. Yield: 70% (199 mg). Anal. calculated for $\text{Cu}_4\text{O}_{12}\text{C}_{48}\text{H}_{56}$: C, 53.4; H, 5.2. Found: C, 53.6; H, 5.0.

2.4. Kinetics of the oxidation of 3,5-di-tert-butylcatechol

In a typical experiment, $\text{Cu}_4(\text{bnac})_4(\mu\text{-OEt})_4$ ($0.85 \times 10^{-4}\text{ mol dm}^{-3}$), 3,5-DTBCH₂ ($8.50 \times 10^{-3}\text{ mol dm}^{-3}$) and the appropriate pyridine ($1.70 \times 10^{-3}\text{ mol dm}^{-3}$) were dissolved in 30 cm^3 of ethanol, under argon atmosphere in a thermostated reaction vessel with an inlet for taking samples

with a syringe. The solution was then heated to the appropriate temperature (40°C), the argon was replaced by air and the oxidation of 3,5-DTBCH₂ was followed spectrophotometrically by monitoring the formation of 3,5-DTBQ at 400.5 nm ($\log \epsilon = 3.21$) as function of time (λ_{max} of a typical band of 3,5-DTBQ).

2.5. X-ray structure determination of

$\text{Cu}_4(\text{bnac})_4(\mu\text{-OEt})_4$

Single crystals of $\text{Cu}_4(\text{bnac})_4(\mu\text{-OEt})_4$ suitable for an X-ray diffraction study were grown from ethanol upon standing at room temperature for a few days. The intensity data were collected with a Nonius Kappa CCD single-crystal diffractometer using Mo K α radiation ($\lambda = 0.71073\text{ \AA}$) at 298 K. Crystallographic data and details of the structure determination are given in Table 1. SHELX-97 [25,26] was used for structure solution and full matrix least squares refinement on F^2 . Crystal structure has been deposited at the Cambridge Crystallographic Data Centre (Deposition no. CCDC 265083).

Table 1

Summary of the crystallographic data and structure parameters for $\text{Cu}_4(\text{bnac})_4(\mu\text{-OEt})_4$

Formula weight	454.0
Crystal system	Monoclinic
Crystal description	Dark green prism
Space group	C2/c
Unit cell dimensions	
<i>a</i> (Å)	13.3980(2)
<i>b</i> (Å)	14.6080(2)
<i>c</i> (Å)	25.7460(4)
α (°)	90.00
β (°)	103.4090(10)
γ (°)	90.00
Volume (Å ³)	4901.59(13)
<i>Z</i>	8
Calculated density (g cm ⁻³)	1.230
Crystal size (mm ³)	0.3 × 0.15 × 0.15
Index ranges	
	$0 \leq h \leq 19$
	$0 \leq k \leq 20$
	$-25 \leq l \leq 25$
Temperature (K)	293(2)
Radiation	Mo K α ($\lambda = 0.71073$)
Absorption coefficient (mm ⁻¹)	0.922
<i>F</i> (000)	1912
Reflections collected	6149
Observed reflections	4419
[<i>I</i> > 2 σ (<i>I</i>)]	
Goodness-of-fit	1.132
Final <i>R</i> indices	$R_1 = 0.0688^a$, $wR_2 = 0.2083^b$
<i>R</i> indices (all data)	$R_1 = 0.0969$, $wR_2 = 0.2264$
Largest difference (peak/hole)	0.744/−0.591

$$^a R = \sum ||F_0| - |F_c|| / \sum |F_0|$$

$$^b R_w = [\sum w(|F_0| - |F_c|)^2 / \sum w|F_0|^2]^{1/2}$$

3. Results and discussion

3.1. Spectroscopic and single crystal X-ray structural characterization

3.1.1. FT-IR and UV-vis

Complex $\text{Cu}_4(\text{bnac})_4(\mu\text{-OEt})_4$ shows absorption bands in the region of 250–330 nm in the electronic spectrum. For the tetranuclear complex the absorption at 322 nm can be assigned to a $(\mu\text{-alkoxo}) \rightarrow \text{Cu}(\text{II})$, ligand to metal charge-transfer transition (LMCT) that typically appears in the 300–400 nm region [27]. Another CT band was also observed at 256 nm and can be attributed to $\text{O} \rightarrow \text{Cu}(\text{II})$ transfer. In addition, one weaker and partially resolved band can be found in the visible region near 665 nm. The presence of the d–d band in this region is consistent with the co-ordination geometry close to square pyramidal for the $\text{Cu}(\text{II})$ center.

Infrared spectra shows two strong bands, 1589 and 1517 cm^{-1} for complex $\text{Cu}_4(\text{bnac})_4(\mu\text{-OEt})_4$, that can be assigned to $\nu(\text{C}=\text{O})$ and $\nu(\text{C}=\text{C})$, respectively. The corresponding peaks in $\text{Cu}(\text{acac})_2$ were observed at 1578 and 1528 cm^{-1} [28–31], thus indicating that the π -system of the asymmetric bnac ligands is somewhat disturbed compared to $\text{Cu}(\text{acac})_2$.

3.1.2. X-ray structure

$\text{Cu}_4(\text{bnac})_4(\mu\text{-OEt})_4$: An ORTEP plot showing the atomic-numbering scheme employed is given in Fig. 1.

This complex is a dimer of dimer and connecting ethoxo-bridges are located between the four copper centers. Each copper(II) ion is in a distorted square pyramidal environment ($\tau = 0.04$ [32]) with two ethoxo-bridged oxygen atoms and two oxygen atoms of bnac occupying the basal plane and another ethoxo group in the apical position with the significantly longer bond length of $2.402(4) \text{ \AA}$. The average $\text{Cu} \cdots \text{Cu}$ distance is 2.99 \AA . Bond distances and angles within the bnac ligand are comparable to those previously reported [33], although larger $\text{O}(2)\text{-Cu}(1)\text{-O}(1) = 93.63(17)^\circ$

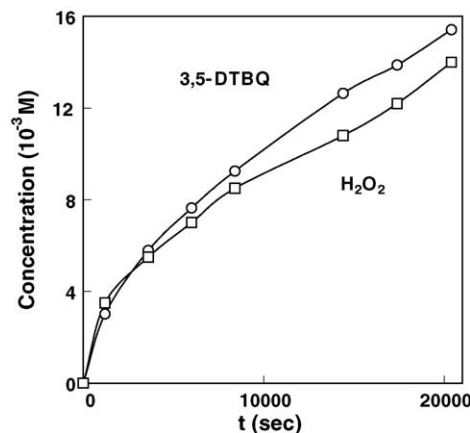


Fig. 2. The oxidation of 3,5-DTBCH₂ catalyzed by $\text{Cu}_4(\text{bnac})_4(\mu\text{-OEt})_4$ in the presence of pyridine. Conditions: $[\text{Cu}_4(\text{bnac})_4(\mu\text{-OEt})_4] = 5.00 \times 10^{-4} \text{ mol dm}^{-3}$ and $[3,5\text{-DTBCH}_2] = 4.90 \times 10^{-2} \text{ mol dm}^{-3}$ under air at 40°C in EtOH.

and smaller $\text{Cu}(1)\text{-O}(1)\text{-C}(7) = 126.0(4)^\circ$ and $\text{Cu}(1)\text{-O}(2)\text{-C}(9) = 125.2(4)^\circ$ angles were observed. Selected bond lengths and bond angles of the complex are listed in Table 2.

3.2. Kinetic studies

The catalytic oxidation of 3,5-di-*tert*-butylcatechol has been studied as a model reaction for the catecholase activity of tyrosinase and catechol oxidase. Complex $\text{Cu}_4(\text{bnac})_4(\mu\text{-OEt})_4$ in the absence and also in the presence of 4-substituted pyridine derivatives was suitable catalyst for the catalytic oxidation of 3,5-DTBCH₂ to 3,5-DTBQ with dioxygen at ambient conditions in relatively good yields. According to parallel electron spectroscopic and iodometric measurements (Fig. 2), the stoichiometry of oxidation reactions corresponds to Eq. (1). No other oxidation products could be detected.

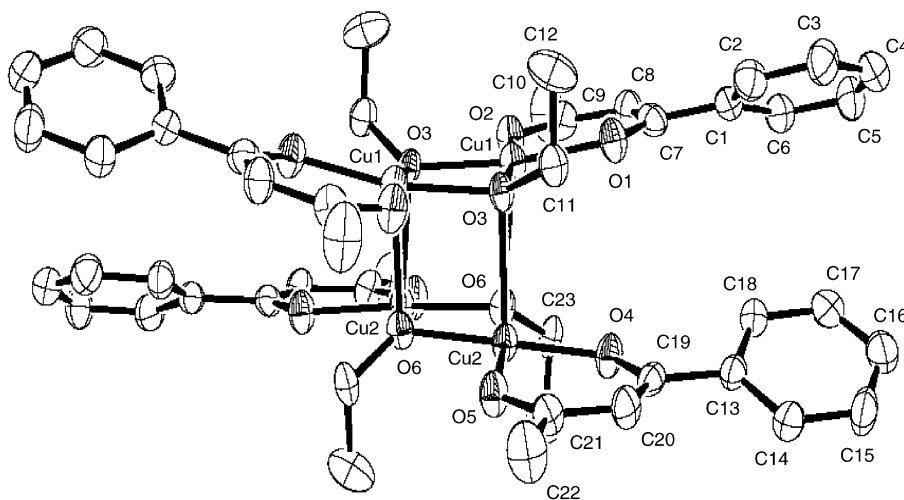


Fig. 1. Ellipsoid drawing of $\text{Cu}_4(\text{bnac})_4(\mu\text{-OEt})_4$ with the atom numbering scheme.

Table 2
Selected bond lengths (Å) and bond angles (°) for $\text{Cu}_4(\text{bnac})_4(\mu\text{-OEt})_4$

Cu(1)–O(1)	1.916(4)	Cu(1)–O(2)	1.908(4)
Cu(1)–O(3)	1.936(3)	Cu(1)–O(3)	1.961(4)
Cu(1)–O(6)	2.402(4)	Cu(1)–Cu(1)	2.9934(12)
Cu(2)–O(4)	1.911(4)	Cu(2)–O(5)	1.915(4)
Cu(2)–O(6)	1.957(3)	Cu(2)–O(3)	2.400(4)
Cu(2)–Cu(2)	2.9789(13)	O(1)–C(7)	1.272(6)
O(2)–C(9)	1.275(7)	O(3)–C(11)	1.452(7)
O(3)–Cu(1)	1.961(4)	O(4)–C(19)	1.271(7)
O(5)–C(21)	1.256(7)	O(6)–C(23)	1.412(6)
O(6)–Cu(2)	1.942(4)	C(1)–C(2)	1.389(9)
C(1)–C(6)	1.394(9)	C(1)–C(7)	1.494(9)
O(2)–Cu(1)–O(1)	93.63(17)	O(2)–Cu(1)–O(3)	172.31(16)
O(1)–Cu(1)–O(3)	94.05(16)	O(2)–Cu(1)–O(3)	93.01(16)
O(1)–Cu(1)–O(6)	167.95(18)	O(3)–Cu(1)–O(3)	79.37(16)
O(2)–Cu(1)–O(6)	96.13(17)	O(1)–Cu(1)–O(6)	105.78(18)
O(3)–Cu(1)–O(6)	82.12(14)	O(3)–Cu(1)–O(6)	83.48(15)
O(2)–Cu(1)–Cu(1)	132.36(13)	O(1)–Cu(1)–Cu(1)	132.28(12)
O(3)–Cu(1)–Cu(1)	40.12(11)	O(3)–Cu(1)–Cu(1)	39.51(10)
O(6)–Cu(1)–Cu(1)	84.20(8)	O(4)–Cu(2)–O(5)	93.21(18)
O(4)–Cu(2)–O(6)	172.76(16)	O(5)–Cu(2)–O(6)	93.25(16)
O(4)–Cu(2)–O(6)	93.06(17)	O(5)–Cu(2)–O(6)	170.14(18)
O(6)–Cu(2)–O(6)	80.11(16)	O(4)–Cu(2)–O(3)	97.57(17)
O(5)–Cu(2)–O(3)	104.92(17)	O(6)–Cu(2)–O(3)	83.91(15)
O(4)–Cu(2)–Cu(2)	132.59(12)	O(5)–Cu(2)–Cu(2)	132.37(13)
O(6)–Cu(2)–Cu(2)	40.36(10)	O(6)–Cu(2)–Cu(2)	40.01(11)
O(3)–Cu(2)–Cu(2)	84.09(8)	Cu(1)–O(3)–Cu(2)	97.96(15)
Cu(2)–O(6)–Cu(1)	97.33(15)	Cu(2)–O(6)–Cu(2)	99.64(16)

The kinetic studies on the oxidation of 3,5-DTBCH₂ were carried out by the method of initial rates by monitoring the increase in the characteristic quinone (3,5-DTBQ) absorption band at 400.5 nm as a function of time. The reactivity studies were performed in ethanol solution at 40 °C. $\text{Cu}_4(\text{bnac})_4(\mu\text{-OEt})_4$ solutions ($0.85 \times 10^{-4} \text{ mol dm}^{-3}$) were treated with 100 equiv. of 3,5-DTBCH₂ in the presence of 20 equiv. of 4-substituted pyridine derivatives. Fig. 3 shows the absorbance versus wavelength spectra of $\text{Cu}_4(\text{bnac})_4(\mu\text{-OEt})_4$ in the presence of 4Me₂N-pyridine after 180 min (85%; TON of

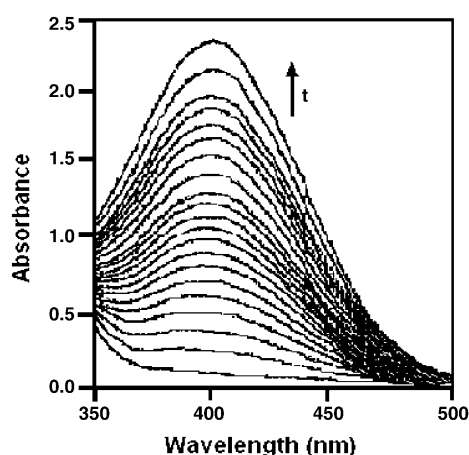


Fig. 3. UV-vis spectra of the oxidation of 3,5-DTBCH₂ by O₂ catalyzed by $[\text{Cu}_4(\text{bnac})_4(\mu\text{-OEt})_4]$. Conditions: $[\text{Cu}_4(\text{bnac})_4(\mu\text{-OEt})_4] = 0.85 \times 10^{-4} \text{ mol dm}^{-3}$, $[3,5\text{-DTBCH}_2] = 8.50 \times 10^{-3} \text{ mol dm}^{-3}$ and $[4\text{Me}_2\text{Npy}] = 1.70 \times 10^{-3} \text{ mol dm}^{-3}$, under air at 40 °C in EtOH.

85.2). The first apparent result over the first 100 min is a significant difference on the reactivities in the presence of various pyridines (Table 3).

In the absence of pyridines complex $\text{Cu}_4(\text{bnac})_4(\mu\text{-OEt})_4$ exhibits a negligibly low catecholase activity (TON of 8.2 after 100 min). The significant acceleration of the catechol oxidation upon addition of pyridine as a Lewis base reveals a significant push effect (Fig. 4). However, pyridine (without catalyst) and 2,6-di-*tert*-butylpyridine in the presence of catalyst had no significant effect, thus showing that the pyridine was not acting simply as a Brønsted base (Fig. 5). The reaction rate dependence on the $\text{Cu}_4(\text{bnac})_4(\mu\text{-OEt})_4$ concentration in the presence of pyridine (Cu:py = 1:20) supports the one half catalyst dependence in the kinetic rate equation indicating a dissociative step from the tetramer to a dimeric species (Fig. 6 and Scheme 1).

Table 3
Hammett σ values and kinetic properties for $\text{Cu}_4(\text{bnac})_4(\mu\text{-OEt})_4$ in the presence of substituted pyridines

Ligand	σ	Reaction time (min)	V_0 (10^6 s^{-1})	Conversion (%)	TON
–	–	100	–	8.2	8.2
4Me ₂ N-py	–0.83	100	1.21	66.4	66.4
H ₂ N-py	–0.66	100	1.27	67.8	67.8
4Ph-py	–0.01	100	0.75	45.8	45.8
py	0	100	0.43	23.8	23.8
4OAc-py	0.50	100	0.38	22.4	22.4
4CN-py	0.66	100	0.26	16.9	16.9

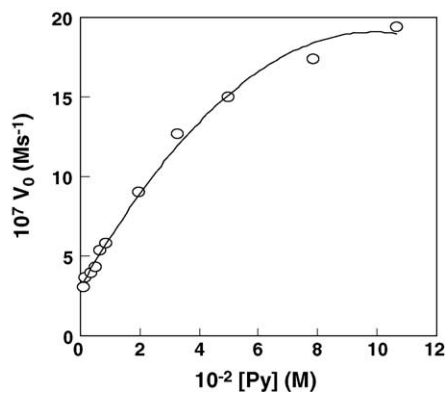


Fig. 4. Dependence of the reaction rates on the pyridine concentrations for the oxidation reaction catalyzed by $\text{Cu}_4(\text{bnac})_4(\mu\text{-OEt})_4$. Conditions: $[\text{Cu}_4(\text{bnac})_4(\mu\text{-OEt})_4] = 0.85 \times 10^{-4} \text{ mol dm}^{-3}$ and $[\text{3,5-DTBCH}_2] = 8.50 \times 10^{-3} \text{ M}$ under air at 40°C in EtOH.

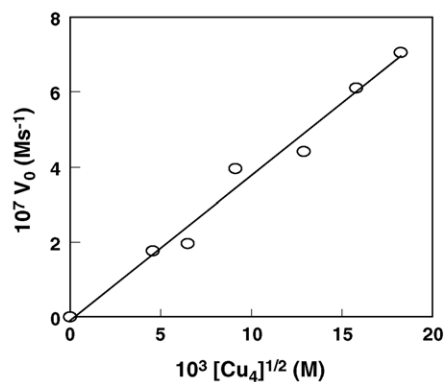


Fig. 6. Dependence of the reaction rates on the $\text{Cu}_4(\text{bnac})_4(\mu\text{-OEt})_4$ concentrations for the oxidation reaction of 3,5-DTBCH₂ in the presence of 20 equiv. pyridine. Conditions: $[\text{3,5-DTBCH}_2] = 8.50 \times 10^{-3} \text{ mol dm}^{-3}$ under air at 40°C in EtOH.

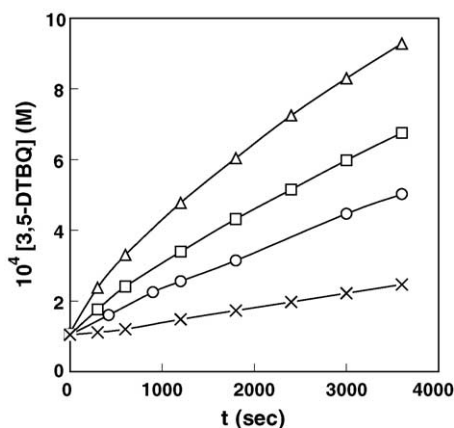
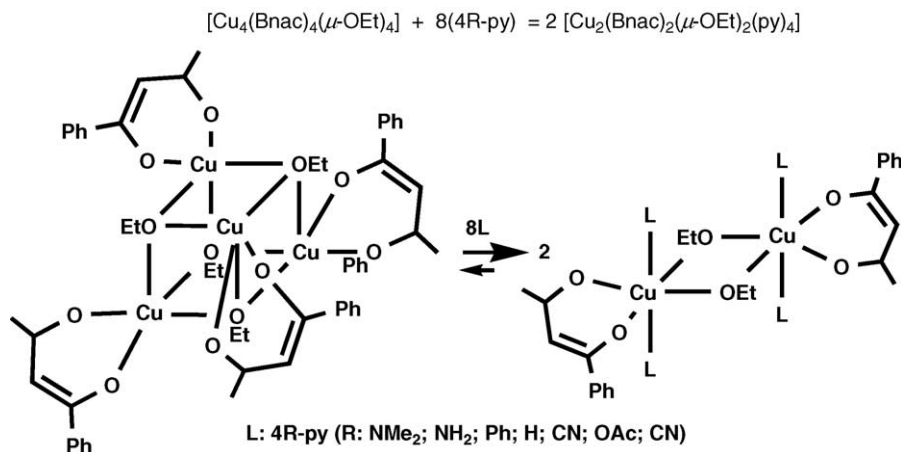


Fig. 5. The oxidation of 3,5-DTBCH₂ catalyzed by $\text{Cu}_4(\text{bnac})_4(\mu\text{-OEt})_4$: (x) in the presence of py (20 equiv.) without catalyst; (O) in the presence of $\text{Cu}_4(\text{bnac})_4(\mu\text{-OEt})_4$ without pyridine; (□) in the presence of $\text{Cu}_4(\text{bnac})_4(\mu\text{-OEt})_4$ with 2,6-di-*tert*-butylpyridine (20 equiv.); (Δ) in the presence of $\text{Cu}_4(\text{bnac})_4(\mu\text{-OEt})_4$ with pyridine (20 equiv.) under air at 40°C in EtOH.

To determine the dependence of the rates on the substrate concentration, solutions of the complex $\text{Cu}_4(\text{bnac})_4(\mu\text{-OEt})_4$ in the presence of excess of pyridine were treated with increasing amounts of 3,5-DTBCH₂. Under this experimental condition, saturation kinetics was found for the initial rates versus the 3,5-DTBCH₂ concentrations (Fig. 7). An analysis of the data based on the Michaelis–Menten model, originally developed for enzyme kinetics, was applied. The results evaluated from Lineweaver–Burk plots are $V_{\text{max}} = 5.10 \times 10^{-7} \text{ mol dm}^{-3} \text{ s}^{-1}$, $K_{\text{M}} = 8.80 \times 10^{-3} \text{ mol dm}^{-3}$, $k_{\text{cat}} = 5.66 \times 10^{-3} \text{ s}^{-1}$ and $k_2(k_{\text{cat}}/K_{\text{M}}) = 0.64 \text{ mol}^{-1} \text{ dm}^{-3} \text{ s}^{-1}$. The turnover rate of 20.4 h^{-1} is comparable to those values reported by Krebs and co-workers [11] ($4\text{--}214 \text{ h}^{-1}$), but significantly lower than the value reported by Monzani et al. [14] with $k_{\text{cat}} = 1188 \text{ h}^{-1}$. In case of our systems, the $\text{Cu} \cdots \text{Cu}$ distance is likely to be around 3.0 \AA , which allows a bridging catechol co-ordination compatible with the distance between the two *o*-diphenol oxygen atoms [10]. Fig. 8 is an other proof for the catechol co-ordination. By adding non-oxidizable catechol such as tetrachlorocatechol into the reaction mixture during



Scheme 1.

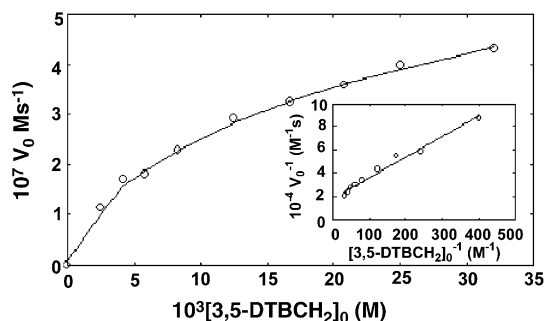


Fig. 7. Dependence of the reaction rates on the 3,5-DTBCH₂ concentrations for the oxidation reaction catalyzed by Cu₄(bnac)₄(μ-OEt)₄. Inset: Lineweaver–Burk plots. The reactions were performed in ethanol [Cu₄(bnac)₄(μ-OEt)₄]=0.85 × 10⁻⁴ mol dm⁻³, [py]=1.70 × 10⁻³ mol dm⁻³ and [3,5-DTBCH₂]=8.50 × 10⁻³ mol dm⁻³ under air at 40 °C.

the oxidation of 3,5-DTBCH₂ the reaction was stopped, supporting the inhibition effect of the Cl₄CH₂ [34–35].

Carrying out the kinetic experiments with Cu₄(bnac)₄(μ-OEt)₄ by varying the dioxygen pressure, first-order dependence was found for the dioxygen concentration (Fig. 9).

As shown in Fig. 10, linear Hammett correlation with ρ value of -0.45 is obtained for the series of 4-substituted pyridines, demonstrating that electron-releasing groups enhance the catechol oxidation.

On the bases of the kinetic data the proposed mechanism assumes a fast irreversible reduction of the in situ forming Cu₂^{II}(bnac)₂(μ-OEt)₂(py)₄ complex by 3,5-DTBCH₂ to Cu(I)⋯Cu(I) followed by the formation of the dicopper dioxygen complex Cu(II)(O₂)Cu(II) in a fast pre-equilibrium, which reacts then with 3,5-DTBCH₂ in the rate-determining step to the starting dicopper(I) species and the products 3,5-DTBQ and H₂O₂, respectively.

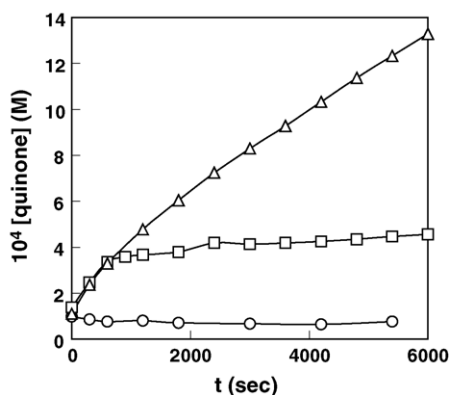


Fig. 8. Oxidation of catechols catalyzed by Cu₄(bnac)₄(μ-OEt)₄. Conditions: (O) [Cu₄(bnac)₄(μ-OEt)₄]=0.85 × 10⁻⁴ mol dm⁻³, [py]=1.70 × 10⁻³ mol dm⁻³ and [Cl₄CH₂]=8.50 × 10⁻³ mol dm⁻³; (□) [Cu₄(bnac)₄(μ-OEt)₄]=0.85 × 10⁻⁴ mol dm⁻³, [py]=1.70 × 10⁻³ mol dm⁻³, [3,5-DTBCH₂]=8.50 × 10⁻³ mol dm⁻³ and [Cl₄CH₂]=8.50 × 10⁻³ mol dm⁻³ after 600 s; (Δ) [Cu₄(bnac)₄(μ-OEt)₄]=0.85 × 10⁻⁴ mol dm⁻³, [py]=1.70 × 10⁻³ mol dm⁻³ and [3,5-DTBCH₂]=8.50 × 10⁻³ mol dm⁻³ under air at 40 °C in EtOH.

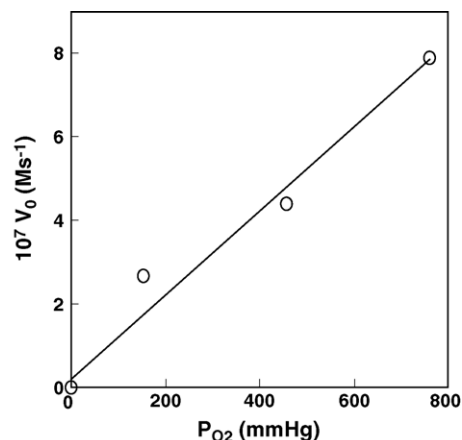


Fig. 9. Dependence of the reaction rates on the dioxygen pressure. Conditions: [Cu₄(bnac)₄(μ-OEt)₄]=0.85 × 10⁻⁴ mol dm⁻³, [py]=1.70 × 10⁻³ mol dm⁻³ and [3,5-DTBCH₂]=8.50 × 10⁻³ mol dm⁻³ at 40 °C in EtOH.

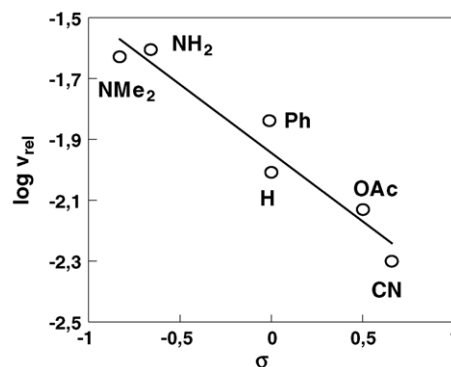


Fig. 10. Plot of log(relative initial rate) vs. σ for the oxidation of 3,5-DTBCH₂ by Cu₄(bnac)₄(μ-OEt)₄ in the presence of 4R-py under air at 40 °C.

4. Conclusion

It has been assumed that geometry around the copper ions, intermetallic distance, lability of exogenous ligands and electrochemical properties are the main key factors that determine the catecholase-like activity of the complexes. In case of our system, the Cu⋯Cu distance is likely to be around 3.0 Å which allows a bridging catechol co-ordination compatible with the distance between the two *o*-diphenol oxygen atoms [10]. Our present systematic investigation shows that the electron density on the copper centers influenced by the nature of axial ligands has a profound effect on the catecholase activity.

Acknowledgment

We thank the Hungarian National Research Fund (OTKA T 043414) for financial support of this work.

References

- [1] L.I. Simándi, Catalytic Activation of Dioxygen by Metal Complexes, Kluwer, Dordrecht, 1992.
- [2] K.A. Magnus, B. Hazes, H. Ton-That, C. Bonaventura, J. Bonaventura, W.G.J. Hol, Proteins Struct. Funct. Genet. 19 (1994) 302.
- [3] E.I. Solomon, U.M. Sundaram, J.E. Carpenter, Chem. Rev. 96 (1996) 2563.
- [4] E.I. Solomon, P. Chen, M. Metz, S.-K. Lee, A.E. Palme, Angew. Chem. Int. Ed. 40 (2001) 4570.
- [5] M. Trémolières, J.B. Bieth, Phytochemistry 23 (1984) 501.
- [6] T. Klabunde, C. Eicken, J.C. Sacchettini, B. Krebs, Nat. Struct. Biol. 5 (1998) 1084.
- [7] R. Than, A.A. Feldman, B. Krebs, Coord. Chem. Rev. 182 (1999) 211.
- [8] C. Gerdemann, C. Eicken, B. Krebs, Acc. Chem. Res. 35 (2002) 183.
- [9] D. Meiwes, B. Ross, M. Kiesshauer, K. Camman, H. Witzel, M. Knoll, M. Borchardt, C. Sandermaier, Lab. Med. 15 (1992) 24.
- [10] C. Eicken, F. Zippel, K. Büldt-Karentzopoulos, B. Krebs, FEBS Lett. 436 (1998) 293.
- [11] P. Gentschev, N. Möller, B. Krebs, J. Inorg. Chim. Acta 300 (2000) 442.
- [12] J. Reim, B. Krebs, J. Chem. Soc., Dalton Trans. (1997) 3793.
- [13] L.M. Berreau, S. Mahapatra, J.A. Halfen, R.P. Hauser, V.G. Young, W.B. Tolman, Angew. Chem. Int. Ed. Engl. 38 (1999) 207.
- [14] E. Monzani, L. Quinti, A. Perotti, L. Casella, M. Gullitti, L. Randaccio, S. Geremia, G. Nardin, P. Faleschini, G. Tabbi, Inorg. Chem. 37 (1998) 553.
- [15] F. Zippel, F. Ahlers, R. Werner, W. Haase, H.-F. Nolting, B. Krebs, Inorg. Chem. 35 (1996) 3409.
- [16] G. Speier, New J. Chem. 18 (1994) 143.
- [17] G. Speier, S. Tisza, Z. Tyeklár, C.W. Lang, C.G. Pierpont, Inorg. Chem. 33 (1994) 2041.
- [18] G. Speier, J. Mol. Catal. 37 (1986) 259.
- [19] J. Kaizer, J. Pap, G. Speier, L. Párkányi, L. Korecz, A. Rockenbauer, J. Inorg. Biochem. 91 (2002) 190.
- [20] K. Selmeczi, M. Reglier, M. Giorgi, G. Speier, Coord. Chem. Rev. 245 (2003) 191.
- [21] A. Llobet, A.E. Martel, M.A. Martinez, J. Mol. Catal. A 129 (1998) 19.
- [22] D.F. Shriver, M.A. Drezdson, The Manipulation of Air-sensitive Compounds, Wiley, New York, 1986.
- [23] D.D. Perrin, W.L. Armarego, D.R. Perrin, Purification of Laboratory Chemicals, 2nd ed., Pergamon Press, New York, 1990.
- [24] R.W. Adams, E. Bishop, R.L. Martin, G. Winter, Aust. J. Chem. 19 (1966) 207.
- [25] G.M. Sheldrick, Acta Crystallogr. A 46 (1990) 467.
- [26] G.M. Sheldrick, SHELXL97. Program for the Refinement of Crystal Structures, University of Göttingen, Germany, 1997.
- [27] H. Adams, N.A. Bailey, I.A. Campbell, Q. He, D.E. Fenton, J. Chem. Soc., Dalton Trans. (1996) 2233.
- [28] H. Junge, H. Musso, Spectrochim. Acta 24A (1968) 1219.
- [29] K. Nakamoto, Infrared and Raman Spectra of Inorganic and Coordination Compounds, 4th ed., Wiley/Interscience, New York, 1986.
- [30] K. Nakamoto, A.E. Martell, J. Chem. Phys. 32 (1960) 588.
- [31] M. Mikami, I. Nakagawa, T. Shimanouchi, Spectrochim. Acta 23A (1967) 1037.
- [32] A.W. Addison, T.N. Rao, J. Reedijk, J. Van Rijn, G.C. Verschoor, J. Chem. Soc., Dalton Trans. (1984) 1350.
- [33] A.W. Addison, P.J. Burke, K. Henrick, T.N. Rao, E. Sinn, Inorg. Chem. 22 (1983) 3645.
- [34] C.G. Pierpont, C.W. Lange, Prog. Inorg. Chem. 44 (1994) 331.
- [35] K.D. Karlin, Y. Gultneh, T. Nicholson, J. Zubieta, Inorg. Chem. 24 (1985) 3725.